

EXPLORING ENHANCED PLASMA PERFORMANCE AFTER PELLET INJECTIONS VIA ROTATIONAL TRANSFORM MODULATION IN THE TJ-II STELLARATOR

I. GARCÍA-CORTÉS¹, K.J. MCCARTHY¹, B. van MILLIGEN¹, T. ESTRADA¹, D. MEDINA-ROQUE¹, A. BACIERO¹, B.A. CARRERAS^{2,3}, A. CAPPA¹, A.A. CHMYGA⁴, J.M FONTDECABA¹, L. GARCIA², R. GARCÍA¹, J. HERNÁNDEZ-SÁNCHEZ¹, F.J. HERNANZ¹, A.S. KOZACHEK³, F. LAPAYESE¹, D. LOPEZ-BRUNA¹, B. LOPEZ-MIRANDA¹, F. MEDINA¹, J.L. de PABLOS¹, N. PANADERO¹, I. PASTOR¹, A. de la PEÑA¹, P. PONS-VILLALONGA¹, M.C. RODRIGUEZ¹, D. TAFALLA¹, V. TRIBALDOS² and TJ-II TEAM¹

¹Laboratorio Nacional de Fusión, Ciemat, Madrid, Spain

²Universidad Carlos III de Madrid, Leganés, Madrid, Spain

³Department of Physics, University of Alaska, Fairbanks, Alaska

⁴Institute of Plasma Physics, NSC KIPT, Kharkov, Ukraine

Email: Isabel.garciacortes@ciemat.es

1. INTRODUCTION

Pellet injection (PI) not only achieves core plasma fuelling but can also induce improved confinement in both tokamak and stellarator devices [1-3]. In the stellarator TJ-II, a sustained pellet-induced enhanced-confinement (PiEC) phase is reached in NBI-heated discharges [4, 5]. Such plasmas show up to 50% increase in performance when compared to the ISS04 scaling law [6] and record values for diamagnetic energy, central electron density, as well as for central and normalized β , are attained for TJ-II plasmas when multiple pellets are injected [5]. Discharges are also characterized by a peaked density profile, reduced turbulence, stronger negative E_r 's from the edge region to the core, and by increased post-injection ion temperatures, the latter being attributed to reduced ion heat diffusivity and improved ion energy confinement. Although neoclassical simulations can explain part of the enhanced performance [7], resistive MHD turbulence [8] and gyrokinetic microturbulence [9] have been also suggested to play a role in driving the transition to these scenarios. In this study, we extend the study to a larger database with multi-pellet injection into different plasma conditions and, by modulating the net plasma current, we attempt to understand how specific rational surfaces can influence PiEC dynamics in TJ-II.

2. EXPERIMENTAL RESULTS

During recent TJ-II experimental campaigns, significant efforts have been made to characterize this PiEC phase in different plasma conditions. A significant database has been analysed to identify how deep core fuelling induces a clear enhanced performance in TJ-II NBI plasmas. Figure 1 shows experimental energy confinement time (τ_E) versus the energy confinement time expected from ISS04 scaling law (τ_E^{ISS04}) [6]. For this, NBI heating power is in the range (400 - 900 kW, Co/CNTR), plasma wall conditioning is used (Boron and/or lithium coating) and 3 magnetic configurations are selected: 100_HX_65 with HX = 42, 44, or 48. The PI target density is in the range 1 to $2 \times 10^{19} \text{ m}^{-3}$ and the pellet time sequence is about $\Delta t \approx \tau_E$. Black points are plasmas fuelled by gas-puff and/or wall recycling while colour points are plasma with PI (one, two or three pellets). As found, in TJ-II, core fuelling is a key parameter to induce an enhanced plasma phase. In addition, reduced density and plasma potential fluctuations, as measured by dual Heavy Ion Beam Probe (HIBP) and Doppler Reflectometry (DR), are seen together with high E_r shear in the density gradient region. Figure 2 shows the E_r gradient measured at 2 DR channels: at $\rho = 0.7$ and 0.8 where E_r shear (dE_r/dr) at $\rho = 0.75$ increases after each PI. This maximum lasts for about 10 ms before tending towards the reference level after (20–30) ms. In contrast, multi-pellets keep this E_r shear at maximum level, this being coincident with longer energy confinement times. In the experiments, a clear relationship is found between observed improvement and the evolution of E_r shear in the gradient region. The latter may be associated with a low-order rational located in the same region, suggesting an important role for MHD turbulence in the formation of transport barriers [8, 10]. Next, in order to understand the role of magnetic topology in the PiEC phase, experiments were conducted for series of NBI heating discharges where cryogenic pellets were injected into plasmas with magnetic configuration: 100_48_65. See Fig. 3.

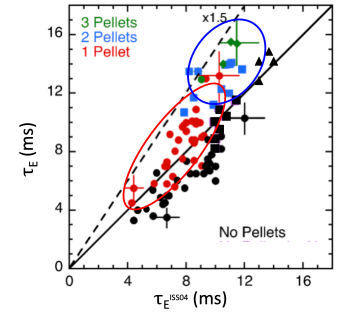


Figure 1: Diamagnetic energy confinement times for selected plasmas, τ_E , versus predicted ISS04 times, τ_E^{ISS04} , as in ref [5]. Data are for different plasmas heating with no PI (black dots) and with 1 (red dots), 2 (blue squares) or 3 (green diamonds) PIs. Error bars are shown for selected data.

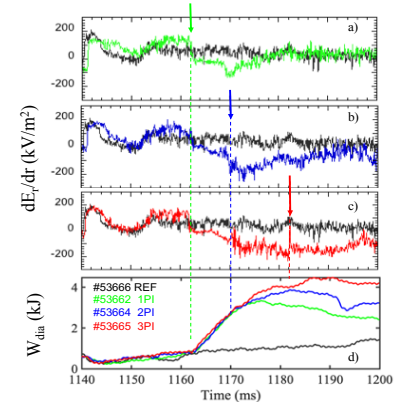


Figure 2: a-c) time evolution for the E_r shear (dE_r/dr) at $\rho = 0.75$ after 1, 2 and 3 PIs, respectively. d) time evolution of stored energy for reference (black), with 1 PI (green), 2 PIs (blue) and 3 PIs (red). All shots in configuration 100_48_65.

For this, the rotational transform profile was systematically varied through external Ohmic coils for a fixed vacuum magnetic configuration with low rational surfaces at or close to the last closed flux surface (LCFS). TJ-II is characterized by its low-shear helical-axis design that means its rotational transform profile can be strongly affected by small variations in net plasma current. In the experiments, the plasma current was varied from -2 kA to +2 kA so specific low-order rational surfaces (e.g., 3/2, 8/5, 5/3) could be placed inside the LCFS. The modified iota-profiles have been obtained based on VMEC calculations for low induced plasma currents [11] (see Fig. 3) and the result is in good agreement with experimental cross-checks by HIBP scans and Mirnov coil analysis and by interpreting structures observed in pellet ablation profiles [12]. In summary, density profiles showed a clear increase in the edge gradient (Fig. 4_left) and a significant confinement improvement for certain induced currents (Fig. 2_Centre). For instance, edge electron density gradients increased by up to 50-60%, while plasma energy content improved by 20-30% when low-order rational surfaces occur about the edge gradient region. DR measurements indicated reduced turbulence levels and enhanced zonal flows in the vicinity of rational surfaces and E_r profiles (Fig. 4_right) displayed systematic variations with plasma current, thereby supporting the hypothesis that these features facilitate transport barrier formation.

Resistive MHD turbulence simulations [8] were carried out for three experimental cases, *i.e.*: positive, negative and near zero plasma currents. The main conclusions are as follows. For positive currents (~ 2 kA) the alignment of the 5/3 rational surface was found to enhance confinement through the formation of dual transport barriers and significant turbulence suppression, accompanied by the generation of strong zonal flows. In contrast, negative currents (~ -2 kA) highlight the interplay between multiple rational surfaces, such as 3/2, 8/5, and 5/3, which improves the confinement by enhancing long-range coupling and further suppressing turbulence. At small currents, the effect of rational surfaces is weak, with limited changes in the rotational transform profile leading to reduced transport barriers and less pronounced confinement improvements.

In summary, we have extend multi-pellet injection studies to a broaden range of plasma conditions. We observe that there exists a clear relationship between observed improvement and the evolution of E_r shear at the gradient region of the 100_48_65 configuration. Furthermore, the impact of the rotational transform profile of TJ-II on the quality of PiEC phases has been analyzed in detail by modulating the net plasma current using external coils. The findings reveal that the radial positioning of low-order rational surfaces near the edge gradient region play a role in the local turbulence suppression, zonal flow generation, and subsequent transport barrier formation. These results are corroborated by Resistive Magneto-Hydrodynamic (MHD) turbulence modeling, offering a qualitative understanding of the experimental observations. This work advances our understanding of magnetic confinement optimization and sets the stage for further exploration of rotational transform dynamics in fusion devices.

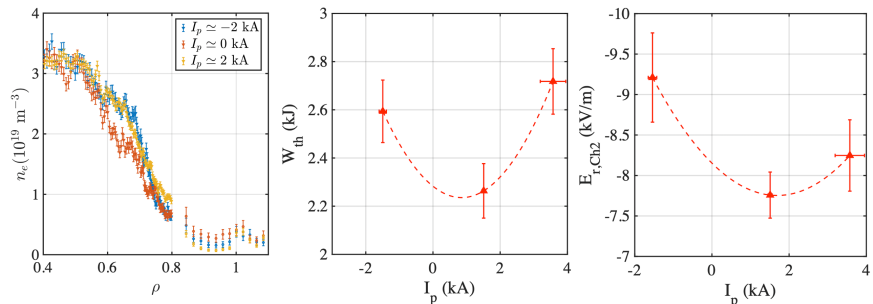


Figure 4. Left: Density profiles measured by Thomson Scattering (TS) and He-beam for different plasma current (blue negative, red near zero, yellow positive). Centre: thermal plasma energy versus I_p . Right: Radial electric field E_r (from Doppler reflectometer channel 2 at $\rho \sim 0.7$ versus I_p . For centre and right figures the dashed lines are meant to guide the eye. The horizontal axis corresponds to the measured value of the plasma current, I_p (kA) at the TS measurement time.

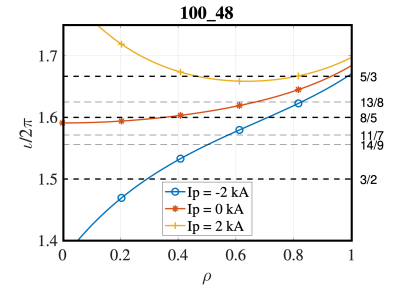


Figure 3: Rotational transform profiles for configuration 100_48_65 in vacuum and for non-zero values of I_p , according to the model of Ref [9]. All rationals $i = n/m$ in the range $1.5 < i < 1.7$ having $n > 15$ are shown as horizontal dashed lines on the right.

REFERENCES

- [1] Lang P.T. *et al* 2018 Nucl. Fusion **58** 036001
- [2] Sakamoto R. *et al* 2001 Nucl. Fusion **41** 381
- [3] Baldzuhn J. *et al* 2020 Plasma Phys. Control. Fusion **62** 055012
- [4] García-Cortés I. *et al* 2023 Phys. Plasmas **30** 072506
- [5] McCarthy K. *et al* 2024 Nucl. Fusion **64** 066019
- [6] Yamada H. *et al* 2005 Nucl. Fusion **45** 1684
- [7] Tribaldos V. *et al* at this conference.
- [8] García L. *et al* 2023 Phys. Plasmas **30** 092303
- [9] García-Regaña J.M. *et al* at this conference.
- [10] López-Bruna D. *et al* 2013 Nucl. Fusion **53** 073051
- [11] Melnikov A. *et al* 2014 Nucl. Fusion **54** 123002
- [12] McCarthy K. *et al* at this conference.